

Experimental Study of Pool Boiling on Metal Block

Tanisha Ajit Muley Anmol Kumar
21110222 22110028

Deepak Soni
22110068

Harsh Kumar Keshri Nikhil Kumar Lal
22110094 22110167

Sanjay Gangotri
22110231

Tapananshu Manoj Gandhi
22110270

Nikhil Kumar Kirtankumar Patel
22110166 22110185

Department of Mechanical Engineering, Indian Institute of Technology Gandhinagar, Gujarat, India

Abstract—This report presents the design, experimental setup, methodology, and analysis for investigating the pool boiling phenomenon on heated metal rods. The study aims to analyze boiling regimes, develop pool boiling curves, and understand heat transfer mechanisms under different conditions of subcooling.

I. INTRODUCTION

Pool boiling is one of the most efficient mechanisms for transferring heat, making it critical for applications like nuclear reactors, electronic cooling, and industrial heat exchangers. The phenomenon involves a sequence of boiling regimes, including nucleate boiling and critical heat flux (CHF), which determine the thermal performance of the system. Investigating these regimes provides a deeper understanding of the thermal and bubble dynamics at play.

This project focuses on analyzing pool boiling on a rectangular aluminum block with dimensions of 20 mm × 30 mm and a length of 10 cm. Unlike the widely studied cylindrical rods, the rectangular geometry offers a novel opportunity to examine variations in heat transfer characteristics and bubble behavior. By using high-resolution imaging and precise temperature monitoring, the experiment aims to develop boiling curves and identify the impact of subcooling and heat flux on CHF.

Through this study, we seek to contribute to the broader knowledge of boiling heat transfer on unconventional geometries, with potential implications for advanced cooling technologies and energy systems.

II. THEORY

When evaporation occurs at the interface between a solid and a liquid, it is known as **boiling**. This process begins when the surface temperature, T_s , surpasses the saturation temperature, T_{sat} , corresponding to the liquid's pressure. Heat flows from the solid surface to the liquid, and Newton's law of cooling can be expressed as:

$$q''_s = h(T_s - T_{sat}) = h\Delta T_e,$$

where $\Delta T_e = T_s - T_{sat}$ is called the *excess temperature*. Boiling is marked by the formation of vapor bubbles, which grow and detach from the surface. The behavior of these bubbles depends on the excess temperature, surface characteristics, and fluid properties such as surface tension.

To better understand the boiling process, it is useful to examine the distinct regimes depicted in the **boiling curve**:

Free Convection Boiling

This occurs when $\Delta T_e > \Delta T_{e,A}$, where $\Delta T_{e,A} \approx 5^\circ\text{C}$. Here, the surface temperature must exceed the saturation temperature enough to support bubble formation. Initially, free convection dominates fluid motion, and bubble formation begins only after reaching a critical excess temperature called the *onset of nucleate boiling (ONB)*.

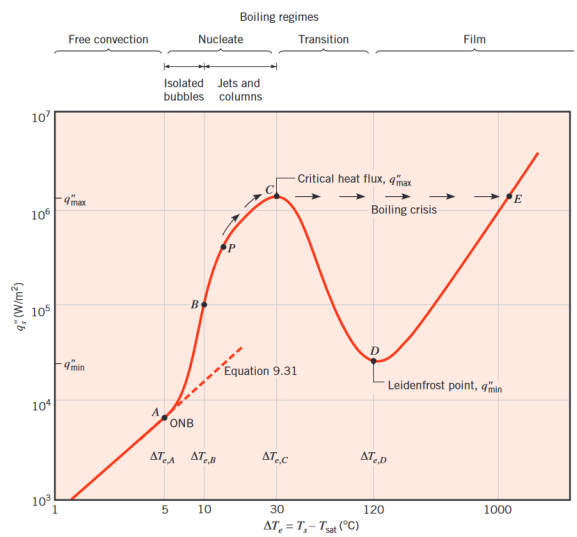


Fig. 1. Pool Boiling Curve For 1 atm.

Nucleate Boiling

Nucleate boiling occurs when $\Delta T_{e,A} \leq \Delta T_e \leq \Delta T_{e,C}$, with $\Delta T_{e,C} \approx 30^\circ\text{C}$. In this regime, two sub-regimes are identified:

- **Region A–B:** Fluid mixing near the surface intensifies, enhancing the heat transfer coefficient (h) and heat flux (q''_s). Heat transfer primarily occurs from the surface to the moving liquid rather than through rising vapor bubbles.
- **Region B–C:** As ΔT_e increases, more nucleation sites become active, leading to greater bubble formation. Bubbles start to interfere and merge, forming vapor jets or slugs.

In the nucleate boiling regime, the boiling curve approximates a straight line on a log–log plot before point P , indicating q''_s is directly proportional to ΔT_e . Beyond point P , the heat flux increases more slowly, eventually peaking at the *critical heat flux*. At this peak, significant vapor formation impedes liquid wetting of the surface. Due to its high heat transfer efficiency, this regime is often preferred for engineering applications.

The occurrence of Critical Heat Flux (CHF) is influenced by the density of nucleation sites and the rate at which bubbles detach from these sites. Mathematical models describing pool boiling behavior have been derived experimentally. The diameter of departing bubbles, D_b , can be determined through a force balance equation where the downward buoyant force is countered by the surface tension. The bubble diameter, D_b , is expressed as:

$$D_b \propto \sqrt{\frac{\sigma}{g(\rho_l - \rho_g)}}$$

Here, σ represents the surface tension, ρ_l and ρ_v correspond to the densities of the liquid and vapor phases of water in the saturated state, respectively, and g denotes the gravitational constant. Additionally, the proportionality constant is influenced by the contact angle between the liquid, its vapor, and the solid surface.

In the boiling curve, the critical heat flux (CHF) represents a significant point. The CHF is important because it marks the maximum heat transfer rate achievable during nucleate boiling before the system transitions into the Transition boiling regime. Beyond this point, the liquid can no longer effectively wet the surface due to the formation of a vapor film, leading to a drastic reduction in heat transfer efficiency. This can result in overheating or failure of the heating surface, making it crucial to understand and predict the CHF for the safe and efficient design of boiling systems. Using dimensional analysis and hydrodynamic stability analysis, a mathematical expression for CHF can be derived as:

$$q''_{max} = Ch_{fg}\rho_v \left[\frac{\sigma g(\rho_l - \rho_v)}{\rho_v^2} \right]^{\frac{1}{4}}$$

The above expression is independent of surface material. For large horizontal cylinders, spheres, and large finite heated surfaces, the value of the constant $C = \frac{\pi}{24} = 0.131$, which is the **Zuber constant**. For large horizontal planes, the value of $C = 0.149$.

Transition Boiling

Transition boiling occurs in the range $\Delta T_{e,C} \leq \Delta T_e \leq \Delta T_{e,D}$, where $\Delta T_{e,D} \approx 120^\circ\text{C}$. Bubble formation becomes so rapid that a vapor film begins to form over the surface. Depending on local conditions, parts of the surface may alternate between nucleate and film boiling, but the vapor film coverage increases with higher ΔT_e . As vapor has much lower thermal conductivity than liquid, the heat transfer coefficient (h) and heat flux (q''_s) decline as ΔT_e rises.

Minimum Heat Flux: The point of minimum heat flux on

the boiling curve is known as the **Leidenfrost point**, which corresponds to the formation of a stable vapor layer. If the heat flux drops below this minimum, the vapor film will collapse, allowing the surface to cool and reinvoke nucleate boiling. The theory used to derive this expression is as follows:

$$q''_{min} = Ch_{fg}\rho_v \left[\frac{\sigma g(\rho_l - \rho_v)}{(\rho_l + \rho_v)^2} \right]^{\frac{1}{4}}$$

Where $C = 0.09$

Film Boiling

Film boiling begins at $\Delta T_e \geq \Delta T_{e,D}$. At the *Leidenfrost point* (point D on the boiling curve), heat flux reaches a minimum, and the surface is entirely covered by a vapor layer. Heat transfer occurs through conduction and radiation across the vapor film. As the surface temperature increases further, radiation effects become more significant, causing the heat flux to rise with increasing ΔT_e .

III. PROBLEM STATEMENT

The phenomenon of pool boiling is characterized by its ability to efficiently transfer heat through distinct boiling regimes, culminating in the critical heat flux (CHF) point. While cylindrical rods are traditionally used for such studies, this project seeks to extend the understanding of pool boiling to a rectangular aluminum block.

The key objective is to design and implement an experimental setup to observe and quantify the pool boiling behavior on an aluminum block with a cross-section of 20 mm × 30 mm and a length of 10 cm. The setup includes:

- A water bath with an immersion heater to control the pool water temperature.
- A cartridge heater embedded in the block for consistent heat input.
- Thermocouples for precise surface temperature measurement.
- A high-resolution microscope camera and LED lighting for real-time visualization of bubble dynamics.

The project will focus on:

- 1) Developing pool boiling curves for three water temperature conditions.
- 2) Visualizing boiling regimes, including nucleate boiling, transition boiling, and film boiling.
- 3) Measuring critical heat flux (CHF) for each condition.
- 4) Analyzing deviations and limitations in achieving the full boiling curve, if any.

The insights gained from this experiment will contribute to the optimization of heat transfer systems and expand the understanding of boiling phenomena on non-cylindrical geometries.

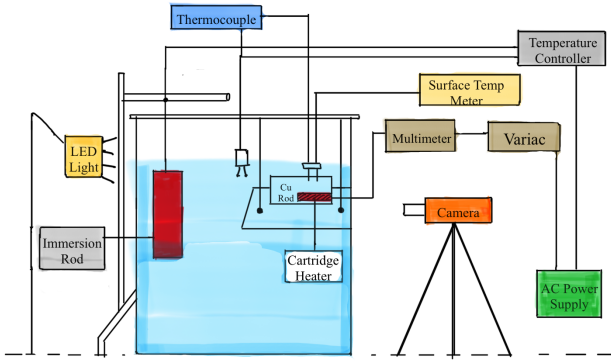


Fig. 2. Schematic diagram of the experimental setup, showing components like the LED light, immersion rod, cartridge heater, copper rod, thermocouple, surface temperature meter, and temperature controller.[NOT TO SCALE], (just for basic idea)

IV. EXPERIMENTAL SETUP



Fig. 3. Complete Experimental Setup

The experimental setup was constructed on an MDF board of size 1 x 2 feet, divided into three sections from left to right. Below is the detailed explanation of each section:

A. Readings Section

This section houses:

- **Thermocouple display:** Shows the water bath temperature and surface temperature of the specimen.
- **Energy meter:** Displays the power consumed by the cartridge heater.

The thermocouple probes originate from this section and extend to the main testing region.



Fig. 4. Readings Section: Thermocouple Display and Energy Meter

B. Main Testing Region

This section, identified by its orange background, contains:

- **2000 ml beaker:** Houses the aluminum testing specimen and the main testing fluid, distilled water.
- **Specimen:** Aluminum block (10mm x 20mm x 100mm) with an embedded cartridge heater sealed using thermal paste and silicone. The surface roughness of the aluminum specimen was measured to be approximately 0.9 Ra. A flat surface was specifically selected for the specimen to enable better visualization of boiling phenomena, ensuring clear observation of bubble formation and detachment during the experiment.
- **Acrylic pillars:** Support and house wires and thermocouple probes:
 - Left pillar: Organizes yellow wire for the cartridge heater and blue thermocouple wires for temperature measurements.
 - Right pillar: Organizes black wire for the immersion rod and grey thermocouple wire for the temperature switch.
- **Glass wool:** Placed below the beaker for insulation.

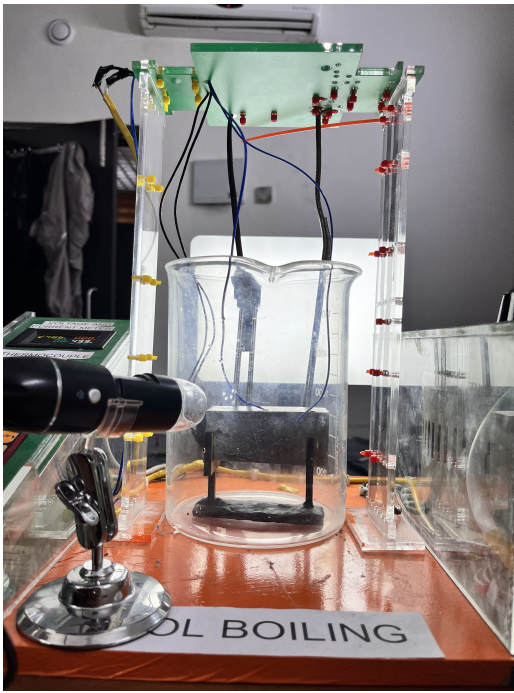


Fig. 5. Main Testing Region: Beaker, Specimen, and Pillars

C. User Input Section

This section allows user control over the system and includes:

- Variac:** Adjusts voltage supplied to the cartridge heater.
- Temperature switch:** Controls the immersion rod to heat the water bath to a desired temperature.
- Adjustable light:** Provides illumination for the testing region, with adjustable brightness and temperature.
- Microscope camera:** 1700x zoom for observing surface phenomena during testing.



Fig. 6. User Input Section: Variac, Temperature Switch, and Control Devices

D. Wiring Arrangement

The setup's wiring is color-coded for clarity:

- Yellow wire:** Runs from the variac (User Input Section) to the cartridge heater (Main Testing Region).
- Blue wires:** Run from the thermocouple display (Readings Section) to the probes measuring water bath and surface temperature.
- Grey thermocouple wire:** Runs from the thermocouple display (Readings Section) to the temperature switch (User Input Section).
- Black wire:** Runs from the immersion rod (Main Testing Region) to the temperature switch (User Input Section).

All wires entering the water are waterproof and securely sealed. Wires are neatly organized and secured using zip ties.

E. Main Setup Overview

The complete setup requires four AC power supplies:

- One for the light.
- One for the variac.
- One for the temperature switch.
- One for the energy meter.



Fig. 7. input power supply

Component	Specification/Details
MDF Board	Size: 1 x 2 feet
Cartridge Heater	150W, Temperature: 400°C in air
Immersion Rod	250W
Main Testing Specimen	Aluminum Block (10mm x 20mm x 100mm)
Surface Roughness	Approx. 0.9 Ra
Beaker	2000 ml
Testing Fluid	Distilled Water
Variac	Power Range: 20V to 240V
Thermocouple Probes	Blue wires for bath and surface temp
Temperature Switch	Controls immersion rod
Light	Adjustable brightness and temperature
Microscope Camera	1700x Zoom
Power Supply	4 AC supplies

TABLE I
SUMMARY OF EXPERIMENTAL SETUP COMPONENTS

V. METHODOLOGY

The experimental procedure was carried out in a controlled environment using the setup described in the previous section. The main goal of the experiment was to observe the heat

transfer dynamics in a distilled water bath with an aluminum specimen, using a cartridge heater for precise temperature control.

A. Initial Setup and Preparation

The experimental setup was assembled as outlined in the previous section. The distilled water was added to the 2000 ml beaker, and the aluminum specimen was placed inside the beaker. The specimen was an aluminum block with dimensions 10mm x 20mm x 100mm, and it was fitted with a cartridge heater that was sealed with thermal paste and silicone.

- **Immersion Rod Setup:** The immersion rod was used to initially heat the distilled water to the desired starting temperature. This temperature was controlled using a temperature switch connected to the immersion rod. The immersion rod was set to a power level sufficient to raise the temperature of the water to a value near the target temperature for the testing phase.
- **Variac Setup:** The variac was used to control the voltage supplied to the cartridge heater. Once the immersion rod had heated the water bath to the desired temperature, the variac was adjusted to begin heating the aluminum specimen using the cartridge heater.

B. Testing Phase

Once the water bath reached the target temperature, the following steps were carried out:

- **Turn on Cartridge Heater:** After setting the water temperature, the cartridge heater was turned on to maintain the water temperature during the experiment. The power supplied to the cartridge heater was adjusted via the variac for controlled heating of the aluminum specimen.
- **Temperature Monitoring:** The thermocouple probes, connected to the thermocouple display, continuously monitored the water bath temperature and the surface temperature of the aluminum specimen. This real-time data was displayed on the thermocouple display. Temperature readings were noted every 30 seconds throughout the experiment.
- **Power Consumption Monitoring:** The energy meter was used to track the power consumption of the cartridge heater. The power was increased by 15 watts at each interval, and the power data was recorded every 30 seconds along with the temperature readings. This data helped in assessing the amount of heat energy being supplied to the system.
- **Observation Using Microscope Camera:** The microscope camera was used to observe the surface phenomena on the aluminum specimen during heating. It provided high-resolution images of any surface changes that occurred due to the heat exposure.
- **Video Recording:** Continuous video footage was recorded to document the experiment and visually capture any surface phenomena or changes on the aluminum specimen as it was heated.

C. Data Collection and Analysis

Throughout the experiment, the following data were collected for analysis:

- **Temperature Data:** The temperatures of both the water bath and the aluminum specimen were recorded using the thermocouple display. Temperature readings were taken every 30 seconds throughout the experiment.
- **Power Data:** The energy meter provided real-time data on the power consumption of the cartridge heater. The power was increased by 15 watts at each interval, and power data was recorded every 30 seconds alongside the temperature data.
- **Microscopic Observations:** The microscope camera allowed for close inspection of the specimen's surface, capturing any signs of deformation or other phenomena at high magnification (1700x zoom).

D. Procedure for Maintaining Temperature during Testing

- **Maintaining Water Temperature:** The immersion rod was only used to heat the water to the desired starting temperature. Once the water reached the set temperature, the immersion rod was turned off, and the cartridge heater took over to maintain the temperature.
- **Adjusting Cartridge Heater Power:** The voltage to the cartridge heater was adjusted via the variac to maintain a consistent temperature in the specimen. This ensured that the thermal energy input was consistent for accurate measurements.
- **Continuous Monitoring:** The thermocouple probes provided continuous feedback on the temperature of both the water and the specimen, ensuring that no overheating occurred during the experiment.

E. Post-Test Procedure

After completing the testing phase, the following steps were taken:

- **Shut down the Cartridge Heater:** The cartridge heater was turned off once the desired temperature profile was reached.
- **Cool Down Period:** The specimen was allowed to cool down to room temperature to finalize the data collection and ensure that the setup was safe for disassembly.
- **Data Logging and Analysis:** All temperature, power, and observational data were logged in a Google Spreadsheet, which is attached in the Appendix. This included calculating the heat transfer efficiency and comparing theoretical results with observed data.
- **Video Recording:** The video footage was saved as an MP4 file and is also attached in the Appendix.

F. Safety Measures

During the experiment, several safety precautions were followed:

- **Waterproofing:** All wires entering the water were waterproofed and securely sealed to prevent any electrical hazards.

- **Thermal Protection:** Both the immersion rod and cartridge heater were carefully monitored to avoid overheating.
- **Personal Protection:** Standard safety equipment, including heat and current-proof gloves and safety glasses, was used to ensure the safety of the operators.

VI. RESULTS

This section highlights the key findings of our experiment involving pool boiling on aluminum specimens with distilled water as the working fluid. The results include the heat flux versus temperature difference (ΔT) graph and visual observations of the boiling regimes.

A. Heat Flux vs Temperature Difference

The graph of heat flux versus temperature difference (ΔT) was obtained using the following formula:

$$\text{Heat Flux}(q) = \frac{\text{Power Supplied (W)}}{\text{Cross-Sectional Area (m}^2\text{)}}$$

The power was measured directly using the energy meter, and the cross-sectional area corresponds to the aluminum specimen's surface exposed to boiling. The graph demonstrates an increase in heat flux with ΔT until the critical heat flux (CHF) is reached. Beyond CHF, due to the inability to achieve higher surface temperatures, the graph shows no additional regimes and plateaus.

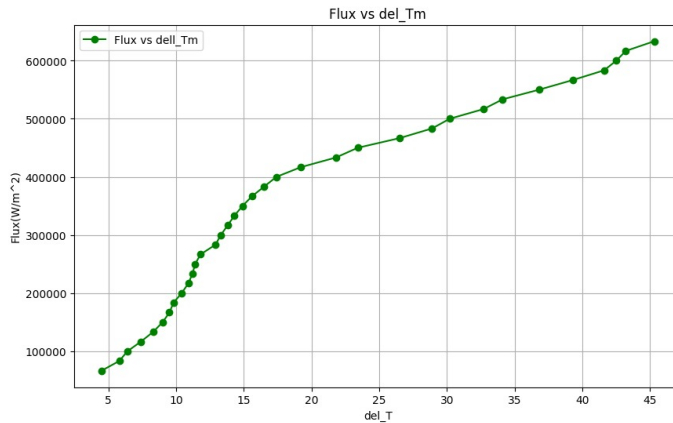


Fig. 8. Heat Flux vs Temperature Difference (ΔT) graph for the aluminum specimen with distilled water.

B. Visual Observation of Boiling Regimes

Distinct boiling regimes were observed during the experiment. However, due to the limitation in achieving higher surface temperatures, the post-CHF regime was not observed. Images were captured to visualize the boiling phenomena up to the CHF regime.

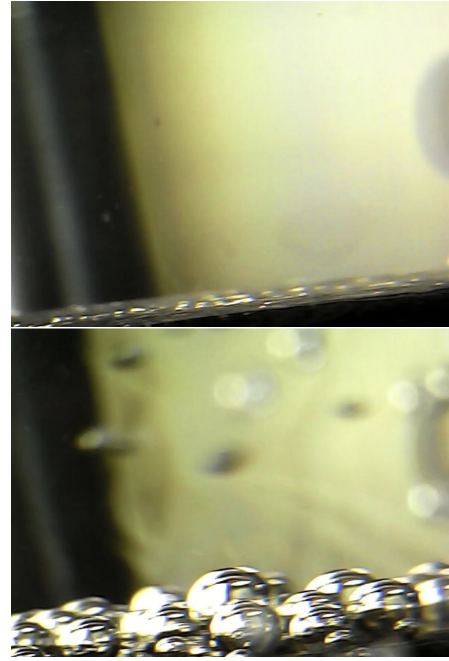


Fig. 9. Boiling regimes for the aluminum specimen with distilled water. Top: Before starting the setup, Bottom: Onset of nucleate boiling.

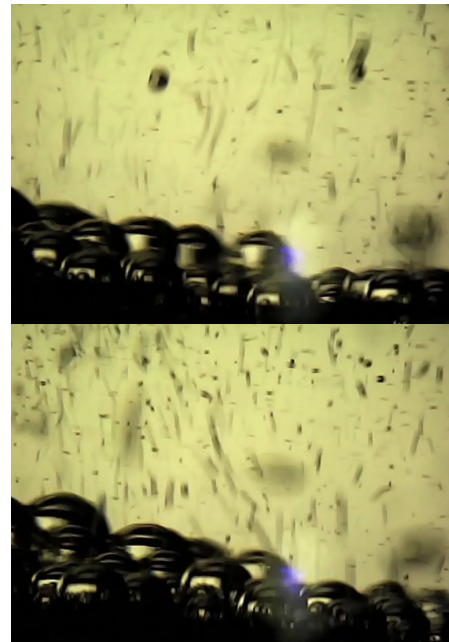


Fig. 10. Boiling regimes for the aluminum specimen with distilled water. Top: Bubble detachment from the surface, Bottom: Rapid bubble formation and detachment, anticipated as CHF.

C. Key Observations

1. **Heat Flux Calculation:** The heat flux was calculated as the ratio of power supplied to the cross-sectional area, with power measured using the energy meter.
2. **Plateau after anticipated CHF:** Due to limitations in achieving higher surface temperatures, the graph did not extend

beyond the CHF, indicating the need for improved heating methods or fluids with lower boiling points to explore further regimes.

3. Visual Regimes: Distinct boiling regimes, including the onset of nucleate boiling, bubble detachment, and rapid bubble formation, were observed and captured. However, the inability to achieve a significant ΔT restricted the visualization of the post-CHF regime.

This section encapsulates the main findings of the experiment while acknowledging the challenges faced during the setup.

VII. ERROR ANALYSIS

The results obtained from the experiment include several sources of potential error that may affect the accuracy of the heat flux calculations and the observation of boiling regimes. The main factors contributing to errors are discussed below:

A. Uncertainty in Temperature Measurements

The measurement of temperature differences (ΔT) relies on precise temperature sensors placed at the heating surface and the surrounding fluid. Any small deviation or calibration error in the thermocouples could lead to inaccuracies in the calculated temperature difference, directly impacting the heat flux calculations. The uncertainty in temperature measurements can result in slight shifts in the position of the boiling curve on the graph.

B. Power Measurement Uncertainty

The power supplied to the heating element was measured using an energy meter. The energy meter has its own calibration uncertainty, which can introduce an error in the measured power values. This, in turn, affects the heat flux calculation, as flux is computed as the power per unit area. Any minor error in power measurement can lead to variations in the flux values, especially at higher temperatures where heat transfer becomes more sensitive to small changes.

C. Cross-Sectional Area Assumption

The heat flux is calculated by dividing the power by the cross-sectional area of the heating surface. In our experiment, we assumed a uniform cross-sectional area. However, if the actual area varies (due to slight surface imperfections or measurement inconsistencies), this assumption introduces error. Small variations in surface area can lead to deviations in the calculated heat flux.

D. Deviation from Theoretical Pool Boiling Curve

To evaluate the experimental data, the theoretical pool boiling curve was compared to the measured data. However, a significant deviation between the two curves was observed, particularly in the region beyond the nucleate boiling regime, where we expected the transition to the critical heat flux (CHF) and the film boiling regime. The inability to achieve the CHF and the lack of a post-CHF regime could be attributed to several factors, including limitations in the setup's heating capacity and fluid properties.

The theoretical pool boiling curve represents the expected heat flux versus temperature difference for a perfect scenario where heat transfer occurs without significant limitations. However, in our setup, the heat flux data plateaus due to the inability of the setup to achieve higher surface temperatures necessary to enter the post-CHF regime.

E. Conclusion

In conclusion, the errors observed in this experiment can primarily be attributed to measurement uncertainties, limitations in the heating setup, and the inherent assumptions made during calculations. Despite these errors, the experiment provided valuable insight into the boiling regimes of the aluminum specimen and the transition from nucleate boiling to CHF.

Further refinements in the setup, such as improving the heating capacity and enhancing temperature measurement accuracy, could lead to a more accurate representation of the theoretical boiling curve, allowing a clearer differentiation between experimental and theoretical data.

VIII. DISCUSSION AND INFERENCE

The pool boiling experiment on aluminum specimens with distilled water as the working fluid provides meaningful insights into heat transfer characteristics and boiling phenomena. The heat flux analysis versus temperature difference (ΔT) and visual observations of boiling regimes highlight important findings.

A. Heat Transfer Characteristics

The heat flux versus temperature difference (ΔT) graph reveals a clear progression of boiling regimes up to the critical heat flux (CHF). The increasing trend in heat flux with ΔT reflects the heat transfer enhancement caused by nucleate boiling, where bubble formation and detachment significantly improve convection by disrupting the thermal boundary layer. The plateau near CHF indicates the system's inability to achieve higher surface temperatures, a common limitation due to material properties or heating constraints.

CHF, the point where heat flux peaks, is crucial for assessing the performance and safety of boiling systems. It underscores the need for material selection and surface treatments to enhance CHF in practical applications. For example, micro-structured or coated surfaces can delay CHF, enabling better thermal management.

B. Visual Observations and Boiling Regimes

Visual observations complement the quantitative data by capturing key boiling stages, such as the onset of nucleate boiling (ONB), bubble detachment, and rapid bubble formation. ONB marks the transition where heat transfer efficiency begins to rise significantly.

However, the experiment's scope was constrained by the inability to reach higher ΔT values beyond CHF. Post-CHF phenomena, like film boiling, were not observed, likely due to the limitations of the heating setup. Overcoming these constraints may require higher energy inputs or fluids with lower boiling points.

C. Implications and Recommendations

This study highlights the following practical implications and areas for improvement:

- **Enhancing CHF:** Surface modifications, such as texturing or hydrophilic coatings, can promote stable bubble dynamics and delay the transition to film boiling, thereby enhancing CHF.
- **Expanding Regime Exploration:** Future experiments could employ advanced heating methods, such as laser or induction heating, to achieve higher temperatures and study post-CHF regimes. Fluids with varying thermo-physical properties, like surfactants or nanofluids, may also broaden the understanding of boiling behaviour.
- **Thermal Management Applications:** These findings highlight boiling as an efficient cooling mechanism for heat exchangers, electronics, and power systems, providing valuable insights for their design and optimization.

IX. CONCLUSIONS

The experiment successfully characterizes boiling behaviour up to CHF, offering a foundation for understanding aluminum-water pool boiling dynamics. While the setup's limitations restricted exploration beyond CHF, the study underscores the importance of surface properties, fluid selection, and heating techniques in boiling performance. Addressing these limitations in future research could unlock deeper insights and practical improvements in boiling systems.

X. NOVELTY

This study explores heat transfer dynamics in pool boiling experiments using distilled water and aluminum as the primary setup. To extend the scope, two additional experiments were conducted, as described below:

A. Experiment 1: Aluminum Specimen with Tap Water

In this variation, the aluminum specimen was retained, but tap water was used as the working fluid instead of distilled water. The experimental procedure was similar to the primary setup, and the following observations were made:

- Bubble formation occurred at a higher onset temperature compared to distilled water due to the increased presence of dissolved impurities.
- The critical heat flux regime was achieved at a lower ΔT , likely influenced by the thermal properties of tap water.

A graph showing the relationship between heat flux and ΔT for this setup is shown in Figure 11.

Visual observations of the boiling regimes for this setup are captured in Figures 12 (a) and (b).

B. Experiment 2: Cartridge Heater with Tap Water

In this case, the cartridge heater itself acted as the testing specimen, directly immersed in tap water. The heater had a length of 50 mm and a diameter of 10 mm. Due to time constraints, no graphs were plotted for this setup, but qualitative observations were made:

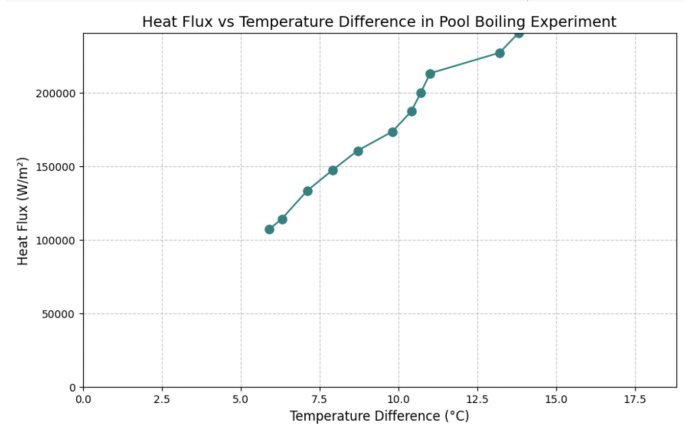


Fig. 11. Heat flux vs. ΔT for the aluminum specimen with tap water.



Fig. 12. Captured images of boiling regimes for the aluminum specimen with tap water. Top: Nucleate boiling regime, Bottom: Critical heat flux regime.

- The bubble formation was concentrated around the heater's surface, indicating localized heat transfer.
- The critical heat flux regime was challenging to quantify due to the lack of real-time graphing, but visual observation confirmed rapid bubble coalescence at higher heat inputs.

Visual observations of the boiling regimes for this setup are captured in Figures 13 (a) and (b).



Fig. 13. Captured images of boiling regimes for the cartridge heater with tap water. Top: Bubble formation near the surface, Bottom: Anticipated Critical heat flux regime.

C. Key Insights from Additional Experiments

The additional experiments with tap water demonstrated the following:

- The dissolved impurities in tap water altered the boiling point, bubble dynamics, and heat transfer efficiency compared to distilled water.
- Using the cartridge heater as the specimen provided insights into localized heat transfer behavior but required further testing to capture detailed quantitative data.
- These findings underline the importance of fluid properties and specimen design in pool boiling studies.

XI. CRITICAL ANALYSIS AND CHALLENGES FACED

During the course of the experiment, several challenges were encountered that impacted the results and observations:

- **Achieving High Surface Temperature:** One of the major challenges was the inability to achieve high surface temperatures on the aluminum specimen. As a result, the temperature gradient (ΔT) between the water bath and the specimen remained relatively low. This limited our ability to observe the full range of heat transfer phenomena, particularly beyond the critical heat flux. We hypothesize that using a fluid with a lower boiling temperature could help address this issue by facilitating heat transfer at lower surface temperatures.
- **Bubble Dynamics Recording:** While attempting to record the bubble dynamics on the specimen's surface, the high speed of bubble formation and movement posed a significant challenge. The current microscope camera setup was not able to capture these rapid changes with sufficient clarity and precision. Future upgrades to high-speed imaging equipment are necessary to overcome this limitation.
- **Limited Heat Flux Observations:** Due to the restricted ΔT , the experiment's observations were limited to the critical heat flux region. Beyond this point, the heat flux appeared almost constant, preventing us from fully analyzing the transition and film boiling regimes. This limitation highlights the need for optimization in experimental parameters, such as specimen material, heater power, and fluid properties, to expand the range of measurable heat transfer phenomena.

Despite these challenges, the experiment provided valuable insights into the heat transfer mechanisms and established a strong foundation for further exploration. Addressing these issues in future studies will enable a more comprehensive understanding of the boiling process and associated phenomena.

XII. FUTURE WORK

In future experiments, we plan to extend our study to include materials with varying thermal conductivity, such as copper and stainless steel. This will provide a broader understanding of the heat transfer characteristics and surface phenomena across different metals. Furthermore, we aim to explore the effects of using alternative working fluids, such as ethylene glycol or silicone oil, instead of distilled water. These fluids are expected to exhibit unique thermal behavior, enriching our dataset and analysis.

However, due to time constraints in the current experiment, we could not conduct tests using copper and stainless steel specimens. These tests will be prioritized in subsequent studies to complete the comparative analysis.

The insights gained from these extended experiments will provide valuable data to optimize heat transfer applications in industrial processes and enhance the understanding of thermal fluid dynamics across diverse material and fluid combinations.



Fig. 14. Copper and Stainless steel specimen.

XIII. ACKNOWLEDGEMENTS

We would like to express sincere gratitude to Professor Soumyadip Sett for his valuable guidance and support throughout the development of this project. Special thanks are also extended to teaching assistant Vamshikrishna Poloju for his assistance and helpful insights during the experimental setup phase. Their advice and encouragement have been instrumental in completing this phase of the project successfully.

XIV. CONTRIBUTION

The contributions of each group member to the project are outlined below:

- **Tanisha Ajit Muley (21110222):** Worked on the initial design part of the pool boiling model, helped in making the structure and also worked on visualization aspect, capturing and processing bubble dynamics during the final pool boiling process.
- **Anmol Kumar (22110028):** Contributed to the project by being part of the ideation process and helping with the model development. Worked on drilling the aluminum and steel blocks for cartridge fitting and ensured the work was done precisely. He also assisted in the final experiment and took part in recording the data carefully.
- **Deepak Soni (22110068):** Was responsible for drafting the initial methodology and troubleshooting technical challenges in the setup. Worked in taking the final results of the experiment and also compiled the theoretical part in the final report.
- **Harsh Kumar Keshri (22110094):** Worked on the initial design part of the pool boiling model, helped in making the structure and also worked on visualization aspect, capturing and processing bubble dynamics during the final pool boiling process.
- **Nikhil Kumar Lal (22110167):** Coordinated as the group leader, helped in the material selection and procurement, worked in formatting phase-1 and phase-3 report, curated idea for the experimental setup and worked in making that, deeply involved in the discussion and the science behind it to achieve the best experimental results.

- **Sanjay Gangotri (22110231):** Worked insight into error analysis for phase one and contributed to the theory part and for the observation for the error analysis. In phase three work in the reading part short off and contribute to the reporting part as well.
- **Tapananshu Manoj Gandhi (22110270):** Contributed to designing the schematic diagram and helped set up the Aluminium specimen, heater, and the overall experimental structure. Was actively involved in preparing the report for all phases, creating the presentation, and explaining parts of the experiment in the Phase 2 video.
- **Nikhil Kumar (22110166):** Contributed to the pool boiling experimental project by designing the schematic diagram, assisting with the experimental setup, and participating in both Phase 1 and Phase 2 report submissions. I was responsible for collecting and analyzing data for Phase 1, ensuring accurate documentation, and preparing the presentation and video, focusing on visualizing and communicating the findings effectively.
- **Kirtankumar Patel (22110185):** Contributed to designing experiment setup , and helped set up the aluminium rod, also involved in preparing the report for all phases, In the phase 2, edited the whole video.

XV. REFERENCES

[1] TheChemEngStudent, "Complete Explanation of Pool Boiling For Heat Transfer," YouTube, 2022. [Online]. Available: <https://www.youtube.com/watch?v=cvRP6uYldvg>. [Accessed: September 20, 2024].

[2] T. L. Bergman, A. S. Lavine, F. P. Incropera, and D. P. DeWitt, *Fundamentals of Heat and Mass Transfer*, 7th ed. Hoboken, NJ: Wiley, 2011.

APPENDIX

The raw data collected during the experiment is available at the following link:

- Raw Data Sheet: https://docs.google.com/spreadsheets/d/1Uf8SWFRJsyUl_Nxwe5M-bxDQQkfR74CKS1XpbMcpB2s/edit?usp=sharing

The code used for data analysis and plotting the graphs is available through the following link:

- Colab Code for Graph Plotting: https://colab.research.google.com/drive/1FfIE8DVQ9WUYNC8-EYKiiDMAAn_A60CLv#scrollTo=TJ_WiLiYEJdc